

Lightning declines over shipping lanes following regulation of fuel sulfur emissions

Chris J Wright^a, Joel A Thornton^a, Lyatt Jaeglé^a, Yang Cao^b, Yannian Zhu^b, Jihu Liu^b, Randall Jones II^a, Robert H Holzworth^c, Daniel Rosenfeld^d, Robert Wood^a, Peter Blossey^a, and Daehyun Kim^{a,e}

^aUniversity of Washington, Department of Atmospheric Sciences, Seattle, WA, 98195

^bNanjing University, School of Atmospheric Sciences, Nanjing, China, 210023

^cUniversity of Washington, Department of Earth and Space Sciences, Seattle, WA, 98195

^dThe Hebrew University of Jerusalem, Institute of Earth Sciences, Jerusalem, Israel, 91904

^eSeoul National University, Department of Atmospheric Science, Seoul, South Korea, 08820

Correspondence: Joel A Thornton (joelt@uw.edu)

Abstract. Aerosol interactions with clouds represent a significant uncertainty in our understanding of the Earth system. Deep convective clouds may respond to aerosol perturbations in several ways that have proven difficult to elucidate with observations. Here, we leverage the two busiest maritime shipping lanes in the world, which emit aerosol particles and their precursors into an otherwise relatively clean tropical marine boundary layer, to make headway on the influence of aerosol on deep convective clouds. The recent seven-fold change in allowable fuel sulfur by the International Maritime Organization allows us to test the sensitivity of the lightning to changes in ship plume aerosol size distributions. We find that, across a range of atmospheric thermodynamic conditions, the previously documented enhancement of lightning over the shipping lanes has fallen by over 40%. The enhancement is therefore at least partially aerosol-mediated, a conclusion that is supported by observations of droplet number at cloud base, which show a similar decline over the shipping lane. These results have fundamental implications for our understanding of aerosol-cloud interactions, suggesting that deep convective clouds are impacted by the aerosol number distribution in the remote marine environment.

Introduction

By acting as cloud condensation nuclei (CCN), aerosol particles influence clouds and, in turn, the Earth's energy balance. These aerosol interactions with clouds represent a significant uncertainty in our understanding of the Earth's climate (Boucher et al., 2013). Shipping lanes can be used as a natural experiment to reduce that uncertainty. Fuel combustion by maritime shipping vessels in the open ocean leads to the emission of aerosol particles and associated precursors, such as SO₂, into relatively clean marine air. These emissions can perturb low-level marine stratus cloud droplet number distributions and related macrophysical properties, such as cloud albedo and lifetime, by increasing CCN concentrations (Diamond et al., 2020; Yuan et al., 2022; Durkee et al., 2000; Radke et al., 1989).

Deep convective cloud (DCC) systems, commonly known as cumulonimbus or thunderstorms when lightning is generated, occur throughout the tropics, and are essential to the Earth's water and energy cycles. In the tropics and some mid-latitude regions, the majority of precipitation and extreme weather is associated with DCCs (Feng et al., 2021). However, there is no strong consensus on the mechanisms or magnitudes of aerosol particle impacts on DCCs (Tao et al., 2012; Seinfeld et al., 2016; Igel and van den Heever, 2021; Varble et al., 2023). Thornton et al (Thornton et al., 2017) documented a potential case of persistent maritime aerosol-DCC interactions analogous to the stratocumulus ship tracks, with the discovery of enhancements in lightning located over the two busiest shipping lanes in the world, which pass through the Indian Ocean and South China Sea (Fig. 1). Lightning results from cloud electrification, which in turn requires sufficient updraft velocity, vertical ice fluxes, and super-cooled liquid water in the mixed-phase region of a DCC to induce and sustain charge separation (Takahashi and Miyawaki, 2002; Deierling et al., 2008). Several relevant mechanisms have been proposed by which aerosol

particle could enhance lightning frequency over the polluted shipping corridors, all of which involve additional aerosol particles from ship emissions causing enhanced cloud droplet nucleation (Twomey, 1977), which subsequently leads to either 1) a perturbation to the super-cooled liquid water and ice hydrometeor distributions in the mixed-phase region of DCC (Mansell and Ziegler, 2013; Blossey et al., 2018; Sun et al., 2024); or 2) an increase in the frequency or intensity of deep convection due to changes in the vertical distribution of humidity (Abbott and Cronin, 2021) or heating (Fan et al., 2018; Grabowski and Morrison, 2020). Some combination of 1 or 2 is also possible.

In January 2020, the International Maritime Organization (IMO) reduced the amount of allowable sulfur in fuel by a factor of seven, from 3.5% to 0.5% to curb effects of the maritime shipping industry on air pollution (IMO, 2020). After similar regulations of fuel sulfur content, a study of ship plumes in the Baltic Sea documented a shift in the aerosol size distribution to smaller sizes (Seppälä et al., 2021). Recent analyses of shallow stratocumulus marine clouds over shipping lanes find changes to cloud brightness, droplet number, and droplet size, amounting to a globally averaged radiative forcing perturbation of O(0.1 Wm⁻²) associated with the IMO regulation, presumably due to the shift in aerosol size distribution (Watson-Parris et al., 2022; Yuan et al., 2022; Diamond, 2023).

Given that shallow clouds have exhibited a shift in droplet size distribution since the IMO regulation of sulfur, so too might DCCs, with downstream effects on mixed-phase microphysics, dynamics, and lightning. Here, we investigate how recent changes in ships' fuel sulfur content impact lightning over the shipping lanes in the tropical Indian Ocean and South China Sea. We show that the shipping lane lightning enhancement decreases significantly with the onset of the IMO regulation and that this decrease in lightning is persistent in time across a range of atmospheric conditions. We further show that the mean cloud droplet number concentration of shallow warm

clouds over the Indian Ocean shipping lane was enhanced before the IMO regulation and also exhibits a decrease since the IMO regulation. Finally, we discuss the implications of these results for the mechanisms of shipping lane lightning enhancement and for aerosol particle-DCC interactions generally.

Approach and findings

The Port of Singapore accounts for roughly 20% of the world’s bunkering fuel demand, and the two primary shipping lanes it services—the Indian Ocean and South China Sea (hereafter “the shipping lanes”)—have nearly an order of magnitude higher traffic than other shipping lanes around the world (Figure 1, top panel) (Mao et al., 2022). We show that there is an enhancement in mean absolute lightning stroke density measured by the World Wide Lightning Detection Network (WWLLN) associated with these shipping lanes, consistent with previous work of Thornton et al, updated here for the time period of 2010 to 2019 in Figure 1 (middle panel). Since 2020, when the IMO regulation of sulfur emissions began, absolute lightning stroke density over the shipping lanes has declined by about 1 stroke $\text{km}^{-2} \text{ year}^{-1}$ as indicated by the difference in lightning stroke density between the mean of years 2020-2023 and that of 2010-2019 shown in Figure 1 (bottom panel). While some of the largest absolute declines in lightning since 2020 occur over the shipping lanes, lightning has increased or decreased in other parts of this region as well. As we illustrate below, changes in the dynamic and thermodynamic context for convection over these shipping lanes, as well as potential changes to shipping due to pandemic and other disruption to trade must be taken into account by controlling for variability in the amount and intensity of convection that leads to lightning as well as proxies for ship traffic.

Ship traffic in the vicinity of Singapore, as measured by vessel fuel sales at the Port of Singapore, has been relatively constant or even increased since 2020 (Figure S1) (Port of Singapore, 2024). The disruption by COVID-19 did not obviously decrease activity at the port, seeming only to have briefly slowed the growth of cargo throughput for 2-3 months in 2020 (Gu et al., 2023). Therefore, we focus on controlling for the variability in background meteorological conditions that impact the frequency and intensity of convection, and thus lightning, over the shipping lanes.

We first examine changes in the lightning stroke density enhancement over the shipping lanes using two basic controls on background meteorology: 1) we only sample from times and pixels with precipitating clouds, using IR and radar-calibrated microwave precipitation measurements from integrated multi-satellite retrievals (IMERG) (Huffman et al., 2015; Pradhan and Markonis, 2023; Watters et al., 2023); and 2) we restrict analyses to the specific seasons in each region when conditions for lighting are favorable (November to April in the Indian Ocean; June to November in the South China Sea). Using these two criteria, we composite the lightning observations as a function of distance to the shipping lanes, the center of which we define as the peak in shipping emissions from the EDGAR emissions inventory (see Methods). As shown in Figure 2, mean absolute lightning as a function of distance from the shipping lanes exhibits a clear enhancement over the shipping lane before (pre-IMO), between approximately 150km south to 150km north of the shipping lanes, that has decreased since the regulation (post-IMO) (Figure 2a). Consistent with Figure 1, lightning has also fallen region-wide, particularly to the south of the shipping lanes. Therefore, we next examine whether the change in absolute lightning observed over the shipping lane since 2020 is greater than expected from natural sources of variability.

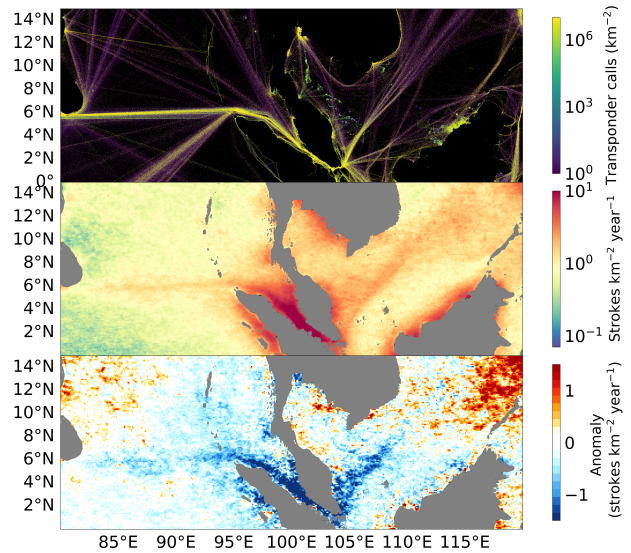


Fig. 1. (top) Map showing the total number of Automatic Identification Systems (AIS) transponder calls from 2015-2021, used by maritime vessels for collision avoidance. Data from the IMF World Seaborne Trade dataset (Cerdeiro et al., 2020). (middle) Climatological mean lightning stroke density near the Port of Singapore (2010-2019). (bottom) Difference of the post-regulation period (2020-2023) lighting stroke density from the 2010-2019 climatology above. See Appendix for further discussion of the retrievals.

To account for inter-annual variability in the frequency and intensity of convection in the region, we construct an estimate of the natural (unperturbed) annual lightning by regressing the observed annual lightning at a given distance from the shipping lane against three variables known to relate to lightning stroke density: Convective Available Potential Energy (CAPE, discussed further below) and precipitation rates (Romps et al., 2018), as well as the annual mean Oceanic Niño Index (ONI), subjected to the same two controls listed above — non-zero precipitation (except ONI) during the high lightning season. The influence of El Niño is assumed to be uniform across the domain for a given year. Inter-annual variability in the MJO was small and had a negligible impact when included in the regression (see SI). The regressed variables explain roughly 33% of variance of the annual means. The regressed predictions for lightning are then subtracted from the observed annual mean, leaving the anomalous mean lightning stroke density, i.e., that which cannot be explained by interannual variability in storm occurrence and intensity, the time series of which is shown as a function of distance from the shipping lane in Figure 2b. The reader is referred to Appendix A for further details about the regression.

Having regressed out natural variations in meteorological drivers of lightning, the annual anomaly in lightning over the shipping lanes prior to 2020 is even more clear, as is the near step-change decrease in the anomaly after 2020. On the right axis of Figure 2b we also show the monthly fraction of fuel sales at the Port of Singapore that are high- and low-sulfur. Prior to the IMO regulation, essentially 100% of fuel sold at the port was the high sulfur type; correspondingly, the lightning anomaly over the shipping lane was 4.0 strokes $\text{km}^{-2} \text{ year}^{-1}$ on average and never fell below 3 strokes $\text{km}^{-2} \text{ year}^{-1}$ for more than one year at a time. Then, as evidenced by the bunkering fuel sales, adoption of the new regulation was immediate in 2020,

such that high sulfur fuel has comprised less than 35% of fuel sold at the Port of Singapore. Total absolute fuel sales have increased since 2020, consistent with overall higher ship traffic (Figure S1); the Port of Singapore also experienced very little attenuation of sales associated with the onset of COVID-19, as noted by studies of port operations (Gu et al., 2023). Since the adoption of lower-sulfur fuels in January 2020, the shipping lane lightning enhancements have declined significantly: the anomaly has fallen to 1.8 strokes $\text{km}^{-2} \text{ year}^{-1}$ on average, with none of the recent 4 years reaching higher than 2.2 strokes $\text{km}^{-2} \text{ year}^{-1}$. That is, the enhancement in lightning over the shipping lane compared to adjacent regions has declined by approximately 50%.

The preceding analysis relies on an assumption that the annual mean CAPE, precipitation, and ONI account for year-to-year variations in the regional drivers of convection and lightning. To further control for higher-frequency natural variations in convective activity and intensity, we examine the lightning enhancement in a 2-dimensional CAPE and precipitation space, using 3-hourly coincident observations of CAPE, precipitation, and lightning. Romps et al. (2018) showed that $\text{CAPE} \times \text{precipitation}$ is a reasonable proxy for lightning frequency over land, and Cheng et al. (2021) showed that, after adjusting for a CAPE threshold, $\text{CAPE} \times \text{precipitation}$ is a reasonable proxy for tropical oceanic lightning frequency. CAPE provides an estimate of the energetic potential for deep convection and the associated updraft strength while precipitation rate indicates both the presence of a storm and a measure of its intensity. By partitioning 3-hourly lightning observations into CAPE and precipitation bins (see Figure 3), we examine how regional and temporal variations in the environmental conditions impact the shipping lane lightning stroke density enhancement. Insofar as they are relevant to lightning generation, 3-hourly CAPE and precipitation observations capture variability from more indirect sources, such as sea surface temperatures (SST), MJO, fronts, etc (see SI for further discussion).

We compute lightning frequency in each CAPE-Precipitation bin using data from a region centered over each shipping lane and from reference regions adjacent to the shipping lanes, similar to those in (Thornton et al., 2017) (see Figure S2). We then compute a relative enhancement in lightning over the shipping lanes, before and after the onset of the IMO regulation, by taking the difference between corresponding CAPE-Precipitation bin-means in the shipping lane and associated reference box. The resulting shipping lane lightning enhancements as a function of both CAPE and Precipitation are shown in Figure 3. Before the IMO regulation (Pre-IMO), a strong shipping lane lightning enhancement existed in nearly every thermodynamic setting (e.g., in each CAPE-Precipitation bin, Figure 3a,d) for both shipping lanes.

Since the IMO regulation (Post-IMO), both shipping lanes exhibit significantly weaker lightning enhancements across most CAPE-Precipitation regimes (Figure 3b,e). The bin-by-bin differences between the Pre and Post-IMO lightning enhancement histograms for each shipping lane are shown in Figure 3 (c and f). For the vast majority of CAPE-Precip bins with statistically significant differences, the lightning enhancement Post-IMO has been weaker than that Pre-IMO. On average across all CAPE-Precip conditions, the lightning enhancement has decreased by 76% and by 47% for the Indian Ocean and South China Sea shipping lanes, respectively.(Figure 3c,f). Thus, for any given thunderstorm sampled, there is less lightning over the shipping lane since 2020 relative to the same type of thunderstorm—i.e., having the same associated CAPE and Precipitation—outside of the shipping lane.

The decline in the lightning enhancement since 2020, which we have illustrated is present even after controlling for potential

natural changes in convective activity or intensity and for relatively constant ship traffic, is therefore most consistent with a change in emissions composition in 2020 associated with the IMO regulation. If decreasing sulfur emissions over the shipping lanes has reduced the total number of viable CCN and disrupted an associated mechanism for lightning enhancement, then there should be a corresponding change in warm cloud microphysics. To further test this hypothesis, we use Moderate Resolution Imaging Spectroradiometer (MODIS) satellite observations of cloud droplet number (N_d) in warm (shallow) clouds over the Indian Ocean shipping lane, where the influence of land is weaker and ship emissions are stronger, during the high-lightning season. The retrievals of N_d follow the method outlined in Zhu et al. (2018), such that we sample only the brightest, most active warm clouds to ensure that assumptions of adiabatic ascent are as realistic as possible (see Appendix A). While we have also examined satellite observations of aerosol optical depth (AOD) over the region, AOD provides limited insights into CCN concentration changes in this region, and especially over the shipping lanes, due to the small size of ship-emitted particles and consequent marginal contributions to AOD (see SI).

Due to the optical thickness of DCC, the retrievals of N_d can only be done for shallow warm clouds. As a result, this analysis samples a different set of conditions than the lightning observations which arise essentially only from DCC. We thus assume that the behavior of N_d in shallow cumulus clouds from the same region is related to, though not necessarily a direct proxy for, N_d at cloud base in DCC. Unlike WLLN lightning observations, which are influenced by the frequency of deep convection and therefore generally trend toward the ITCZ, the N_d retrievals mostly represent perturbations to CCN below shallow cumulus.

In Figure 4, we show that prior to the IMO regulation, there is a clear trend in N_d toward land (north), as aerosol number concentrations are typically greater over land than over oceans (Figure S6), as well as a clear perturbation in N_d over the shipping lane. This N_d perturbation is roughly 10-15% above the average of droplet concentrations 150km north and 150km south, which is similar in magnitude to the shipping lane perturbations to N_d detected by Diamond et al. (2020) in Southeast Atlantic stratocumulus clouds. That the N_d perturbation over the Indian Ocean shipping lane is similar to that in other locations is a significant finding on its own, as observations of persistent, mean-state N_d perturbations by ships are rare (Diamond and Wood, 2020). Since the IMO regulation, the N_d away from the shipping lane mostly maintain their previous levels, as indicated by the overlap in the 95% confidence intervals (shading), particularly to the north. We have partially accounted for variability in aerosol particles using MERRA-2 reanalysis estimates of continental dust and biomass burning aerosol variations across the region in constructing Figure 4. That said, a dearth of aerosol observations in the tropical Pacific likely limit the ability of reanalysis products to capture the full variability in CCN sources, possibly explaining some remaining differences in N_d pre and post IMO over the southern region of the domain.

Most notably in Figure 4, the enhancement in N_d over the shipping lane has become essentially undetectable. The decline in N_d over the shipping lane establishes additional support for the declining lightning enhancement being related to a shift in aerosol particle number-size distributions, and consequently changes to the CCN distributions over the shipping lanes induced by the IMO regulation. It is important to note that N_d derived from shallow cumulus clouds will not be directly proportional to the CCN available for activation in deep convective clouds (DCC), nor to the lightning enhancements that might result from CCN enhancements. Given the strong updrafts that occur in

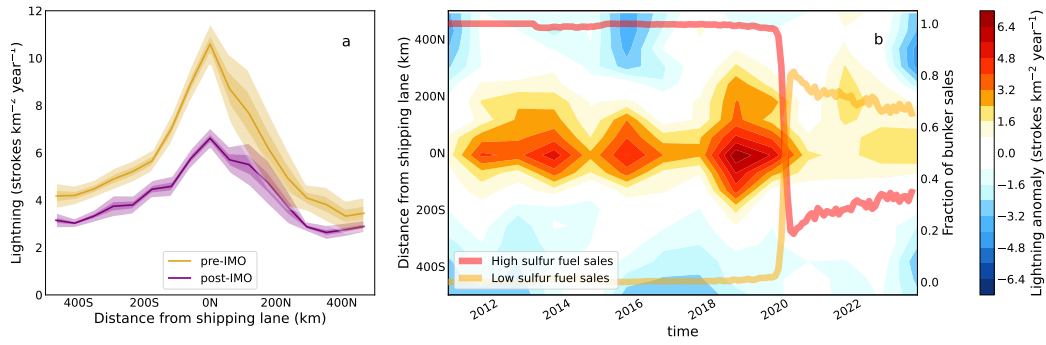


Fig. 2. (a) Lightning stroke density as a function of distance to the shipping lanes before and after the IMO regulation. Shading represents $\pm 2SE$ and $\pm 3SE$ (b) Hovmöller diagram of the annual mean lightning anomaly from the linear regression using Convective Available Potential Energy, precipitation, and Oceanic Niño Index from reanalysis data and observations (see text and SI for more details).

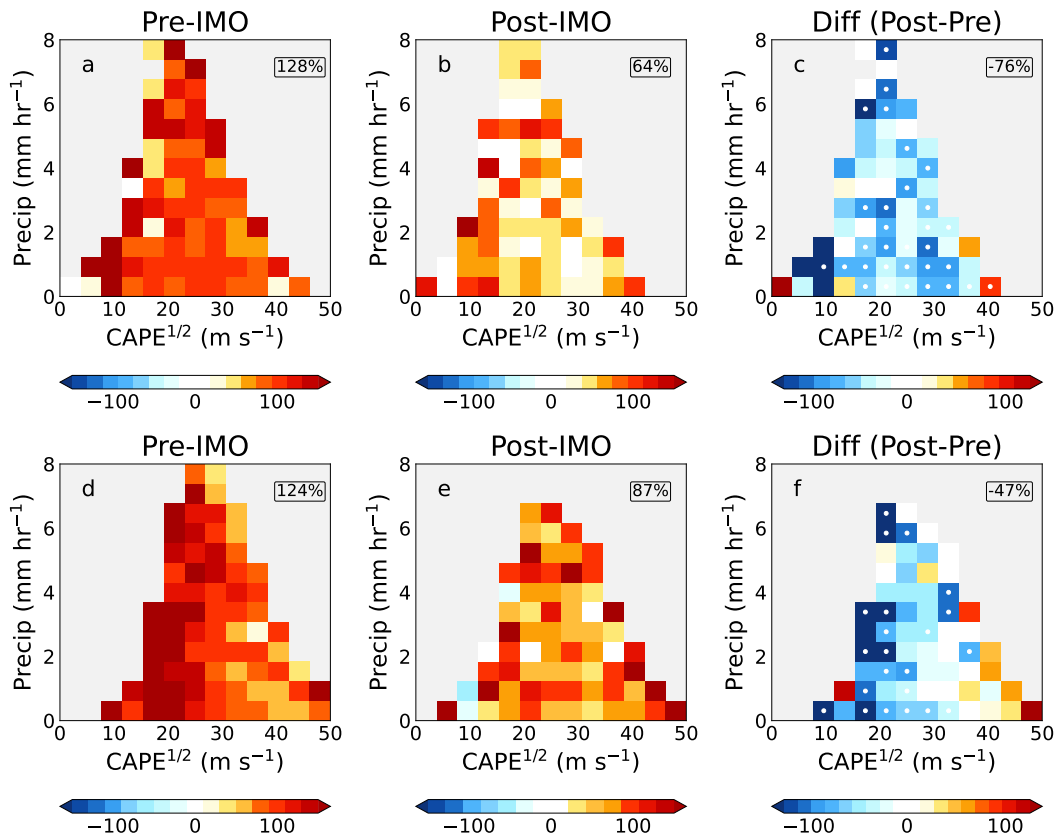


Fig. 3. Mean shipping lane percent enhancement in lightning stroke density (i.e., the relative difference in lightning over the shipping lane from that over immediately adjacent regions, see text), shown as colored pixels, binned by square root of CAPE reanalysis data (x-axis) and precipitation observations (y-axis) for the Indian Ocean (a)–(c) and South China Sea (d)–(f) shipping lanes. Enhancements since the regulation (b, e) are lower than before the regulation (a, d). The difference between post- and pre-IMO periods of the shipping lane lightning enhancements are represented in (c, f), where stippled bins indicate significance (p less than 0.05).

DCC, aerosol particles can experience very high super-saturation with respect to liquid water, enabling smaller, often more numerous ultrafine aerosol (Hobbs et al., 2000) to act as CCN in DCC than can do so in shallow cumulus. The change in N_d is an otherwise rare, observable indication that the IMO regulations have clearly shifted aerosol particle distributions over the shipping lanes of interest here.

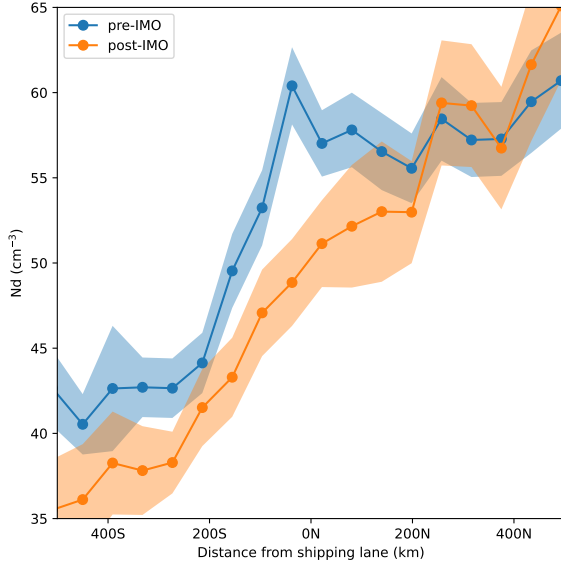


Fig. 4. Warm cloud-base droplet number (N_d) concentrations over the Indian Ocean, derived from MODIS observations of optical depth and effective radius following the procedure from Zhu et al. (2018). The pre-IMO regulation period is 2010-2019. Note the general increasing trend northward through the domain toward greater land influence, and the broad localized enhancement over the shipping lane prior to the regulation. Shading represents $\pm 2SE$.

Implications

We find that a previously identified enhancement in lightning stroke density over the two major shipping routes near the Port of Singapore has declined by over 40% since 2020, when the IMO regulation aimed at reducing sulfur emissions from maritime shipping came into effect. The decline of lightning is evident after controlling for natural variations in environmental conditions that characterize the intensity and frequency of thunderstorms, presented most clearly in Figure 3. While the ships themselves do likely act as attractors of lightning due to their prominence over the flat ocean (Peterson, 2023), there is not evidence of a significant change in the number of ships traversing these shipping lanes over this time period (Figure S1). Further, that there was an independently observed perturbation to N_d over the Indian Ocean shipping lane prior to the IMO regulation that has since nearly vanished is indicative of a coincident change in CCN over the region. The statistically robust decline of the lightning enhancement, alongside the onset of the IMO regulation and observed changes in warm cloud microphysics, suggest that the mechanism for the lightning enhancement is likely induced by ship emissions of aerosol particles and precursors. The concomitant decline of N_d and lightning shown here lends credence to the set of CCN-mediated hypotheses previously proposed for invigoration of lightning (Fan et al., 2018; Abbott and

Cronin, 2021; Mansell and Ziegler, 2013; Grabowski and Morrison, 2020).

Precisely how increases in N_d might lead to enhanced lightning remains unresolved. Both the pre-IMO and post-IMO perturbations to N_d are smaller than the enhancements of lightning. In part, this difference may be explained by the different supersaturation conditions sampled by the N_d and lightning retrievals (warm, trade cumulus and deep convective environments, respectively), which will lead to different portions of the aerosol size distribution that can be activated in each case. Additionally, there may be non-linear relationships between N_d , secondary ice processes, and resulting charge separation; or additional interactions between DCC and aerosol, such as ice nucleation. Thornton et al. showed that DCC over the shipping lane exhibited anomalously higher radar reflectivity in the mixed phase region prior to 2015. While we find a similar indication for the four years prior to the IMO (see Figure S5) using a different satellite-based radar sensor, statistically robust tests of whether there have been changes in DCC reflectivity since the IMO regulation are not yet possible. However, we expect the statistical strength for the comparison between the two periods to increase, enabling a broader assessment of the post-IMO DCC response to maritime shipping emissions in the coming years.

In situ observations of aerosol size distributions, needed to assess how the IMO regulations have led to changes in CCN in these regions, are notably lacking. Seppälä et al. (2021) find that, in the case of a factor of 10 reduction in ship fuel sulfur content, in-plume aerosol size distributions generally shift toward lower sizes and lower total number concentrations (i.e., that the number of ultrafine particles smaller than 50nm increases and the number of particles larger than 50nm decreases substantially). According to the ultrafine invigoration hypothesis proposed in Fan et al. (2018), the increase in small ultrafine particles observed by Seppälä et al. (2021) would buffer enhancement losses of larger CCN, which is inconsistent with the strong decrease in lightning stroke density that we observe. Therefore, we conclude that the lightning enhancement over the shipping lane prior to the IMO regulation was mostly the result of enhancements in relatively larger aerosol particles (e.g. >50 nm in size) that perturbed: 1) cloud microphysics, such as elevated supercooled liquid water concentrations or rime splintering (Mansell and Ziegler, 2013) and/or 2) updraft frequency, by means of heightened free tropospheric humidity or a mesoscale circulation response (Blossey et al., 2018; Grabowski and Morrison, 2020). Enhancements in smaller ultrafine particles may play a role in the small, remaining lightning enhancement that has persisted over the shipping lanes post-IMO.

We use the IMO regulation of ship fuel sulfur to identify and assess connections between maritime shipping emissions associated with international trade, pollution aerosol size and composition, DCC microphysics, and lightning stroke density. Further work combining *in situ* and remote sensing of aerosol and cloud microphysics together with lightning frequency is needed to clarify the mechanisms behind these connections, and to quantify the relative roles of dynamic and microphysical responses. Our findings herein show that these regions remain a useful testbed for understanding aerosol pollution impacts on deep convective clouds and lightning.

Appendix A: Retrievals, data processing, and methods

Lightning stroke density observations come from the Worldwide Lightning Location Network (WWLLN), a ground-based lightning detection network with continuous global coverage of lightning at a resolution of 10km (Dowden et al., 2002). WWLLN uses very low frequency radio impulses (3-30 kHz) that, upon emission from a

lightning stroke, propagates between the Earth-ionosphere waveguide and disperses into a wave train. The phase and frequency of that wave train determine the time of group arrival at three or more measurement stations, which can be used to back out the location of the stroke. While the detection efficiency for individual events is lower than satellite-based methods, continuous observations for more than a decade offer much more statistical power over our region of interest.

We use integrated multi-satellite retrievals for GPM (IMERG) precipitation rates (Huffman et al., 2015) and European Centre for Medium-Range Weather Forecasts (ECMWF) ReAnalysis-5th Generation (ERA5) atmospheric reanalyses (Hersbach et al., 2020) CAPE to compare the enhancement across various thermodynamic conditions. IMERG precipitation combines microwave and radar retrievals from TRMM and the GPM constellation. In ERA5, a value for CAPE is calculated for every departing level between the surface and 350hPa as follows:

$$CAPE = \int_{z_{dep}}^{z_{top}} g \left(\frac{\theta_{ep} - \bar{\theta}_{esat}}{\bar{\theta}_{esat}} \right) dz$$

where z_{dep} is the departing level, z_{top} is the level of neutral buoyancy, θ_{ep} is the virtual potential temperature of the parcel, and $\bar{\theta}_{esat}$ is the saturation virtual potential temperature of the environment. Once CAPE has been calculated for all levels, the most unstable layer is selected. We use $CAPE^{1/2}$, which is directly proportional to w_{max} , the theoretical maximum vertical velocity achievable at a location given the stability of the atmosphere. This follows from the proportionality between kinetic energy and the square of velocity. Further discussion of CAPE as it relates to lightning can be found in (Cheng et al., 2021) and (Romps et al., 2018).

Lightning in Figure 1 is shown on $0.1^\circ \times 0.1^\circ$ grid, calculated from 3-hourly lightning stroke densities. For subsequent calculations of the enhancement (Figures 2-3) all data (CAPE, precipitation, and lightning) is 3-hourly and mapped to a $0.5^\circ N \times 0.625^\circ E$ grid to minimize collocation errors and noise, and for comparison with MERRA-2 aerosol and meteorological reanalysis fields. Smoothly varying data (CAPE) is remapped bilinearly, while non-smoothly varying data (precipitation and lightning) are remapped conservatively (see Staff (2014) and sources therein for further detail on regridding practices). To provide some basic control for thermodynamic and meteorological variability, we only consider precipitating clouds (precipitation greater than 0.1mm/hr) during the high-lightning season (see SI).

We use data from 2010 onward, as WWLLN detection efficiency was still increasing rapidly prior to 2010. The shipping lanes are defined as regions where the Emissions Database for Global Atmospheric Research (EDGAR) $PM_{2.5}$ shipping emissions are greater than $5 \times 10^{-12} \text{ kg m}^{-2} \text{ s}^{-1}$ (Crippa et al., 2016). To remove influence from katabatic flows and sea-breeze driven convergence, we only consider the larger blue regions outlined in Figure S2. This notably removes the straight of Malacca, a region with both very high shipping emissions and active convection. There, surface convergence from land-based precipitation outflows on Sumatra and Malaysia and the adjacent landmasses make it challenging to establish a counterfactual, given the well-known land-ocean contrast in lightning stroke rates Cheng et al. (2021); Romps et al. (2018).

For Figure 2, the lightning stroke density (F) as a function of time (t) and distance from shipping lane (y) from the entire record is regressed as:

$$F(y, t) = \beta * X(y, t) + \epsilon$$

where X is the vector of predictors, CAPE, precipitation, and ONI, β is the vector of coefficients. ϵ is the residual or "anomaly" that is

shown in the figure. This anomaly represents the difference between the lightning one would expect given the environmental conditions ($\beta * X$) (see Figure S3) and the observed lightning (F).

We utilized the "brightest 10%" method (Zhu et al., 2018; Cao et al., 2023) to obtain reliable N_d cloud droplet number concentration retrievals from MODIS Aqua across our target domain from 2010 to 2023. This method involves selecting the brightest 10% of clouds within each scene to calculate N_d values for every $0.5^\circ \times 0.5^\circ$ grid box. The validity of this retrieval method has been corroborated through comparisons with ship-based observations (Efraim et al., 2020; Wang et al., 2021). N_d is computed using the cloud effective radius (r_e) and cloud optical depth (τ), as described by the equation:

$$N_d = \frac{\sqrt{5}}{2\pi k} \left(\frac{f_{ad} C_w \tau}{Q_{ext} \rho_w r_e^5} \right)^{\frac{1}{2}}$$

where k represents the volume radius ratio of cloud droplets (r_v) to re ($k = (r_v/r_e)^3 = 0.8$). The term f_{ad} denotes the adiabatic fraction, for which we assumed a constant value of 1 in our study, due to the absence of more refined alternatives (Bennartz and Rausch, 2017; Grosvenor et al., 2018). C_w signifies the adiabatic cloud water condensation rate within an ascending cloud parcel, expressed in grams per cubic meter per meter ($\text{g m}^{-3} \text{ m}^{-1}$). The extinction efficiency factor, Q_{ext} , is assumed to be 2, and ρ_w is the density of water. To enhance the accuracy of our N_d estimations for each $0.5^\circ \times 0.5^\circ$ grid box, we excluded pixels where the solar zenith angle exceeded 65 degrees (Grosvenor and Wood, 2014). We also excluded of scenes containing mixed-phase, ice, or multilayer clouds. Consequently, after applying these filtering criteria, the remaining dataset comprised less than 1% of multilayer cloud pixels in any given grid. We use only the Indian Ocean shipping lane to maximize signal-to-noise, as the South China Sea has a much weaker signal due to its proximity to land and lower ship emissions. Inclusion of the South China Sea in the analysis does not alter the results. Finally, in order to remove the impact of dust storms advected over the Bay of Bengal, and to thereby reduce interannual variability in N_d outside the shipping lanes, we collocate 3-hourly MERRA-2 aerosol reanalysis output of dust and black carbon with the MODIS N_d retrievals. We then remove any N_d retrievals where dust concentrations increase above 1 ng m^{-3} or black carbon concentrations above 0.1 ng m^{-3} (approximately the 50th percentile in each case).

Data availability

ERA5 CAPE may be downloaded using the Copernicus API at cds.climate.copernicus.eu. IMERG Precipitation and MERRA-2 aerosol are available for download at disc.gsfc.nasa.gov. WWLLN data is available at [WWLLN.net](https://wwlln.net). ONI index is available at psl.noaa.gov/data/correlation/oni.data. Precipitation Feature reflectivity datasets are available for download at: <https://atmos.tamucc.edu/trmm/data/>. MODIS Aqua (MYD06) retrievals are available at ladsweb.modaps.eosdis.nasa.gov. Precipitation Feature reflectivity datasets are available for download at: <https://atmos.tamucc.edu/trmm/data/>. Global ship traffic density is available at: datacatalog.worldbank.org/search/dataset/0037580/Global-Shipping-Traffic-Density. Analysis and plotting available at [10.5281/zenodo.11373991](https://zenodo.org/record/11373991) (Wright, 2024).

Author Contributions

Analysis: CJW. Writing: CJW and JAT. Conceptualization and methodological development: CJW, JAT, LJ, and RW. N_d retrievals

by: YC, YZ, JL. Additional expertise provided by RH, DR, RJ, PN, and DK

Acknowledgements

This work was funded by a grant from the U.S. National Science Foundation (AGS-2113494). Additional funding included (in order of authorship): Natural Science Foundation of China grant 42075093 (YC, YZ, JL), BSF Grant 2020809 (DR), NASA/UMBC grant NASA0144-01 (RW), NSF grant AGS-1912130 (PN), and New Faculty Startup Fund from Seoul National University (DK). The authors wish to thank the World Wide Lightning Location Network (<http://wwlln.net>), a collaboration among over 50 universities and institutions, for providing the lightning location data used in this paper.

Bibliography

- Abbott, T. H. and Cronin, T. W. (2021). Aerosol invigoration of atmospheric convection through increases in humidity. *Science*, 371(6524):83–85. Publisher: American Association for the Advancement of Science.
- Bennartz, R. and Rausch, J. (2017). Global and regional estimates of warm cloud droplet number concentration based on 13 years of AQUA-MODIS observations. *Atmospheric Chemistry and Physics*, 17(16):9815–9836. Publisher: Copernicus GmbH.
- Blosssey, P. N., Bretherton, C. S., Thornton, J. A., and Virts, K. S. (2018). Locally Enhanced Aerosols Over a Shipping Lane Produce Convective Invigoration but Weak Overall Indirect Effects in Cloud-Resolving Simulations. *Geophysical Research Letters*, 45(17):9305–9313. .eprint: <https://onlinelibrary.wiley.com/doi/pdf/10.1029/2018GL078682>.
- Boucher, O., Randall, D., Artaxo, P., Bretherton, C., Feingold, G., Forster, P., Kerminen, V.-M., Kondo, Y., Liao, H., Lohmann, U., Rasch, P., Sathesh, S., Sherwood, S., Stevens, B., and Zhang, X. (2013). Clouds and Aerosols. pages 571–892.
- Cao, Y., Zhu, Y., Wang, M., Rosenfeld, D., Liang, Y., Liu, J., Liu, Z., and Bai, H. (2023). Emission Reductions Significantly Reduce the Hemispheric Contrast in Cloud Droplet Number Concentration in Recent Two Decades. *Journal of Geophysical Research: Atmospheres*, 128(2):e2022JD037417. .eprint: <https://onlinelibrary.wiley.com/doi/pdf/10.1029/2022JD037417>.
- Cerdeiro, Komaromi, Liu, and Saeed (2020). World Seaborne Trade in Real Time: A Proof of Concept for Building AIS-based Nowcasts from Scratch.
- Cheng, W.-Y., Kim, D., and Holzworth, R. H. (2021). CAPE Threshold for Lightning Over the Tropical Ocean. *Journal of Geophysical Research: Atmospheres*, 126(20):e2021JD035621. .eprint: <https://onlinelibrary.wiley.com/doi/pdf/10.1029/2021JD035621>.
- Crippa, M., Janssens-Maenhout, G., Dentener, F., Guizzardi, D., Sindelarova, K., Muntean, M., Van Dingenen, R., and Granier, C. (2016). Forty years of improvements in European air quality: regional policy-industry interactions with global impacts. *Atmospheric Chemistry and Physics*, 16(6):3825–3841. Publisher: Copernicus GmbH.
- Deierling, W., Petersen, W. A., Latham, J., Ellis, S., and Christian, H. J. (2008). The relationship between lightning activity and ice fluxes in thunderstorms. *Journal of Geophysical Research: Atmospheres*, 113(D15). .eprint: <https://onlinelibrary.wiley.com/doi/pdf/10.1029/2007JD009700>.
- Diamond, M. S. (2023). Detection of large-scale cloud microphysical changes within a major shipping corridor after implementation of the International Maritime Organization 2020 fuel sulfur regulations. *Atmospheric Chemistry and Physics*, 23(14):8259–8269. Publisher: Copernicus GmbH.
- Diamond, M. S., Director, H. M., Eastman, R., Possner, A., and Wood, R. (2020). Substantial Cloud Brightening From Shipping in Subtropical Low Clouds. *AGU Advances*, 1(1):e2019AV000111. .eprint: <https://onlinelibrary.wiley.com/doi/pdf/10.1029/2019AV000111>.
- Diamond, M. S. and Wood, R. (2020). Limited Regional Aerosol and Cloud Microphysical Changes Despite Unprecedented Decline in Nitrogen Oxide Pollution During the February 2020 COVID-19 Shutdown in China. *Geophysical Research Letters*, 47(17):e2020GL088913. .eprint: <https://onlinelibrary.wiley.com/doi/pdf/10.1029/2020GL088913>.
- Dowden, R. L., Brundell, J. B., and Rodger, C. J. (2002). VLF lightning location by time of group arrival (TOGA) at multiple sites. *Journal of Atmospheric and Solar-Terrestrial Physics*, 64(7):817–830.
- Durkee, P. A., Noone, K. J., Ferek, R. J., Johnson, D. W., Taylor, J. P., Garrett, T. J., Hobbs, P. V., Hudson, J. G., Bretherton, C. S., Innis, G., Frick, G. M., Hoppel, W. A., O'Dowd, C. D., Russell, L. M., Gasparovic, R., Nielsen, K. E., Tessmer, S. A., Öström, E., Osborne, S. R., Flagan, R. C., Seinfeld, J. H., and Rand, H. (2000). The Impact of Ship-Produced Aerosols on the Microstructure and Albedo of Warm Marine Stratocumulus Clouds: A Test of MAST Hypotheses 1i and 1ii. *Journal of the Atmospheric Sciences*, 57(16):2554–2569. Publisher: American Meteorological Society Section: Journal of the Atmospheric Sciences.
- Efrain, A., Rosenfeld, D., Schmale, J., and Zhu, Y. (2020). Satellite Retrieval of Cloud Condensation Nuclei Concentrations in Marine Stratocumulus by Using Clouds as CCN Chambers. *Journal of Geophysical Research: Atmospheres*, 125(16):e2020JD032409. .eprint: <https://onlinelibrary.wiley.com/doi/pdf/10.1029/2020JD032409>.
- Fan, J., Rosenfeld, D., Zhang, Y., Giangrande, S. E., Li, Z., Machado, L. A. T., Martin, S. T., Yang, Y., Wang, J., Artaxo, P., Barbosa, H. M. J., Braga, R. C., Comstock, J. M., Feng, Z., Gao, W., Gomes, H. B., Mei, F., Pöhlker, C., Pöhlker, M. L., Pöschl, U., and de Souza, R. A. F. (2018). Substantial convection and precipitation enhancements by ultrafine aerosol particles. *Science*, 359(6374):411–418. Publisher: American Association for the Advancement of Science.
- Feng, Z., Leung, L. R., Liu, N., Wang, J., Houze Jr, R. A., Li, J., Hardin, J. C., Chen, D., and Guo, J. (2021). A Global High-Resolution Mesoscale Convective System Database Using Satellite-Derived Cloud Tops, Surface Precipitation, and Tracking. *Journal of Geophysical Research: Atmospheres*, 126(8):e2020JD034202. .eprint: <https://onlinelibrary.wiley.com/doi/pdf/10.1029/2020JD034202>.
- Grabowski, W. W. and Morrison, H. (2020). Do Ultrafine Cloud Condensation Nuclei Invigorate Deep Convection? Section: *Journal of the Atmospheric Sciences*.
- Grosvenor, D. P., Sourdeval, O., Zuidema, P., Ackerman, A., Alexandrov, M. D., Bennartz, R., Boers, R., Cairns, B., Chiu, J. C., Christensen, M., Deneke, H., Diamond, M., Feingold, G., Fridlind, A., Hünerbein, A., Knist, C., Kollias, P., Marshak, A., McCoy, D., Merk, D., Painemal, D., Rausch, J., Rosenfeld, D., Russchenberg, H., Seifert, P., Sinclair, K., Stier, P., van Diedenhoven, B., Wendisch, M., Werner, F., Wood, R., Zhang, Z., and Quaas, J. (2018). Remote Sensing of Droplet Number Concentration in Warm Clouds: A Review of the Current State of Knowledge and Perspectives. *Reviews of Geophysics*, 56(2):409–453. .eprint: <https://onlinelibrary.wiley.com/doi/pdf/10.1029/2017RG000593>.
- Gu, Y., Chen, Y., Wang, X., and Chen, Z. (2023). Impact of COVID-19 epidemic on port operations: Evidence from Asian ports. *Case Studies on Transport Policy*, 12:101014.
- Hersbach, H., Bell, B., Berrisford, P., Hirahara, S., Horányi, A., Muñoz-Sabater, J., Nicolas, J., Peubey, C., Radu, R., Schepers, D., Simmons, A., Soci, C., Abdalla, S., Abellan, X., Balsamo, G., Bechtold, P., Biavati, G., Bidlot, J., Bonavita, M., De Chiara, G., Dahlgren, P., Dee, D., Diamantakis, M., Dragani, R., Flemming, J., Forbes, R., Fuentes, M., Geer, A., Haimberger, L., Healy, S., Hogan, R. J., Hólm, E., Janisková, M., Keeley, S., Laloyaux, P., Lopez, P., Lupu, C., Radnoti, G., de Rosnay, P., Rozum, I., Vamborg, F., Villaume, S., and Thépaut, J.-N. (2020). The ERA5 global reanalysis. *Quarterly Journal of the Royal Meteorological Society*, 146(730):1999–2049. .eprint: <https://onlinelibrary.wiley.com/doi/pdf/10.1002/qj.3803>.
- Hobbs, P. V., Garrett, T. J., Ferek, R. J., Strader, S. R., Hegg, D. A., Frick, G. M., Hoppel, W. A., Gasparovic, R. F., Russell, L. M., Johnson, D. W., O'Dowd, C., Durkee, P. A., Nielsen, K. E., and Innis, G. (2000). Emissions from Ships with respect to Their Effects on Clouds. Section: *Journal of the Atmospheric Sciences*.
- Huffman, G. J., Bolvin, D. T., Braithwaite, D., Hsu, K., Joyce, R., Xie, P., and Yoo, S.-H. (2015). NASA global precipitation measurement (GPM) integrated multi-satellite retrievals for GPM (IMERG). *Algorithm theoretical basis document (ATBD) version*, 4(26):30. Publisher: NASA Goddard Space Flight Center Greenbelt, MD.
- Igel, A. L. and van den Heever, S. C. (2021). Invigoration or Enervation of Convective Clouds by Aerosols? *Geophysical Research Letters*, 48(16):e2021GL093804. .eprint: <https://onlinelibrary.wiley.com/doi/pdf/10.1029/2021GL093804>.
- IMO (2020). IMO 2020 Cutting Sulphur Oxide Emissions.
- Mansell, E. R. and Ziegler, C. L. (2013). Aerosol Effects on Simulated Storm Electrification and Precipitation in a Two-Moment Bulk Microphysics Model. *Journal of the Atmospheric Sciences*, 70(7):2032–2050. Publisher: American Meteorological Society Section: Journal of the Atmospheric Sciences.
- Mao, X., Rutherford, D., Osipova, L., and Georgeff, E. (2022). Exporting emissions: the Port of Singapore. Technical report.
- Peterson, M. (2023). Interactions Between Lightning and Ship Traffic. *Earth and Space Science*, 10(11):e2023EA002926. .eprint: <https://onlinelibrary.wiley.com/doi/pdf/10.1029/2023EA002926>.
- Port of Singapore (2024). Bunkering Statistics.
- Pradhan, R. K. and Markonis, Y. (2023). Performance Evaluation of GPM IMERG Precipitation Products over the Tropical Oceans Using Buoys. *Journal of Hydrometeorology*, 24(10):1755–1770. Publisher: American Meteorological Society Section: Journal of Hydrometeorology.
- Radke, L. F., Coakley, J. A., and King, M. D. (1989). Direct and Remote Sensing Observations of the Effects of Ships on Clouds. *Science*, 246(4934):1146–1149. Publisher: American Association for the Advancement of Science.
- Roms, D. M., Charn, A. B., Holzworth, R. H., Lawrence, W. E., Molinari, J., and Vollaro, D. (2018). CAPE Times P Explains Lightning Over Land But Not the Land-Ocean Contrast. *Geophysical Research Letters*, 45(22):12,623–12,630. .eprint: <https://onlinelibrary.wiley.com/doi/pdf/10.1029/2018GL080267>.
- Seinfeld, J. H., Bretherton, C., Carslaw, K. S., Coe, H., DeMott, P. J., Dunlea, E. J., Feingold, G., Ghan, S., Guenther, A. B., Kahn, R., Kraucunas, I., Kreidenweis, S. M., Molina, M. J., Nenes, A., Penner, J. E., Prather, K. A., Ramanathan, V., Ramaswamy, V., Rasch, P. J., Ravishankara, A. R., Rosenfeld, D., Stephens, G., and Wood, R. (2016). Improving our fundamental understanding of the role of aerosol-cloud interactions in the climate system. *Proceedings of the National Academy of Sciences*, 113(21):5781–5790. Publisher: Proceedings of the National Academy of Sciences.
- Seppälä, S. D., Kuula, J., Hyvärinen, A.-P., Saarikoski, S., Rönkkö, T., Keskinen, J., Jalkanen, J.-P., and Timonen, H. (2021). Effects of marine fuel sulfur restrictions on particle number concentrations and size distributions in ship plumes in the Baltic Sea. *Atmospheric Chemistry and Physics*, 21(4):3215–3234. Publisher: Copernicus GmbH.
- Staff, N. (2014). The Climate Data Guide: Regridding Overview.
- Sun, R., Lu, X., Gao, M., Du, Y., Lin, H., Wright, C., He, C., and Yin, K. (2024). The impacts of shipping emissions on lightning: roles of aerosol-radiation-interactions and aerosol-cloud-interactions. *Environmental Research Letters*, 19(3):034038. Publisher: IOP Publishing.
- Takahashi, T. and Miyawaki, K. (2002). Reexamination of Riming Electrification in a Wind Tunnel. *Journal of the Atmospheric Sciences*, 59(5):1018–1025. Publisher: American Meteorological Society Section: Journal of the Atmospheric Sciences.
- Tao, W.-K., Chen, J.-P., Li, Z., Wang, C., and Zhang, C. (2012). Impact of aerosols on convective clouds and precipitation. *Reviews of Geophysics*, 50(2). .eprint: <https://onlinelibrary.wiley.com/doi/pdf/10.1029/2011RG000369>.
- Thornton, J. A., Virts, K. S., Holzworth, R. H., and Mitchell, T. P. (2017). Lightning enhancement over major oceanic shipping lanes. *Geophysical Research Letters*, 44(17):9102–9111. .eprint: <https://onlinelibrary.wiley.com/doi/pdf/10.1002/2017GL074982>.
- Twomey, S. (1977). The Influence of Pollution on the Shortwave Albedo of Clouds. *Journal of the Atmospheric Sciences*, 34(7):1149–1152. Publisher: American Meteorological Society Section: Journal of the Atmospheric Sciences.
- Varble, A. C., Igel, A. L., Morrison, H., Grabowski, W. W., and Lebo, Z. J. (2023). Opinion: A critical evaluation of the evidence for aerosol invigoration of deep convection. *Atmospheric Chemistry and Physics*, 23(21):13791–13808. Publisher: Copernicus GmbH.
- Wang, Y., Zhu, Y., Wang, M., Rosenfeld, D., Gao, Y., Yao, X., Sheng, L., Efrain, A., and Wang, J. (2021). Validation of satellite-retrieved CCN based on a cruise campaign over the polluted Northwestern Pacific ocean. *Atmospheric Research*, 260:105722.

- Watson-Parris, D., Christensen, M. W., Laurensen, A., Clewley, D., Gryspeerdt, E., and Stier, P. (2022). Shipping regulations lead to large reduction in cloud perturbations. *Proceedings of the National Academy of Sciences*, 119(41):e2206885119. Publisher: Proceedings of the National Academy of Sciences.
- Watters, D. C., Gatlin, P. N., Bolvin, D. T., Huffman, G. J., Joyce, R., Kirstetter, P., Nelkin, E. J., Ringerud, S., Tan, J., Wang, J., and Wolff, D. (2023). Oceanic Validation of IMERG-GMI Version 6 Precipitation Using the GPM Validation Network. *Journal of Hydrometeorology*, 25(1):125–142. Publisher: American Meteorological Society Section: Journal of Hydrometeorology.
- Wright, C. (2024). Lightning Declines Over Shipping Lanes Follow Regulation of Fuel Sulfur: Data Analysis.
- Yuan, T., Song, H., Wood, R., Wang, C., Oreopoulos, L., Platnick, S. E., von Hippel, S., Meyer, K., Light, S., and Wilcox, E. (2022). Global reduction in ship-tracks from sulfur regulations for shipping fuel. *Science Advances*, 8(29):eabn7988. Publisher: American Association for the Advancement of Science.
- Zhu, Y., Rosenfeld, D., and Li, Z. (2018). Under What Conditions Can We Trust Retrieved Cloud Drop Concentrations in Broken Marine Stratocumulus? *Journal of Geophysical Research: Atmospheres*, 123(16):8754–8767. .eprint: <https://onlinelibrary.wiley.com/doi/pdf/10.1029/2017JD028083>.

Supplemental Information

As noted in the main manuscript, fuel sales statistics from the Port of Singapore are a reasonable proxy for the amount of large ship activity in the two shipping lanes considered here. While not accounting for vessels that might fuel elsewhere prior to transiting one of the shipping lanes, it is likely that if a ship transits the Indian Ocean shipping lane to Singapore it will fuel there for a subsequent journey through the South China Sea (or a return to the Indian Ocean) and vice versa for a ship first transiting the South China Sea. Thus, that gross fuel sales for large vessels at the Port of Singapore has remained largely constant or even increased since 2020 (see Figure S1) suggests fairly minimal changes in ship traffic through these two shipping lanes. There is nothing like a 50% drop in shipping that might explain the change in lightning.

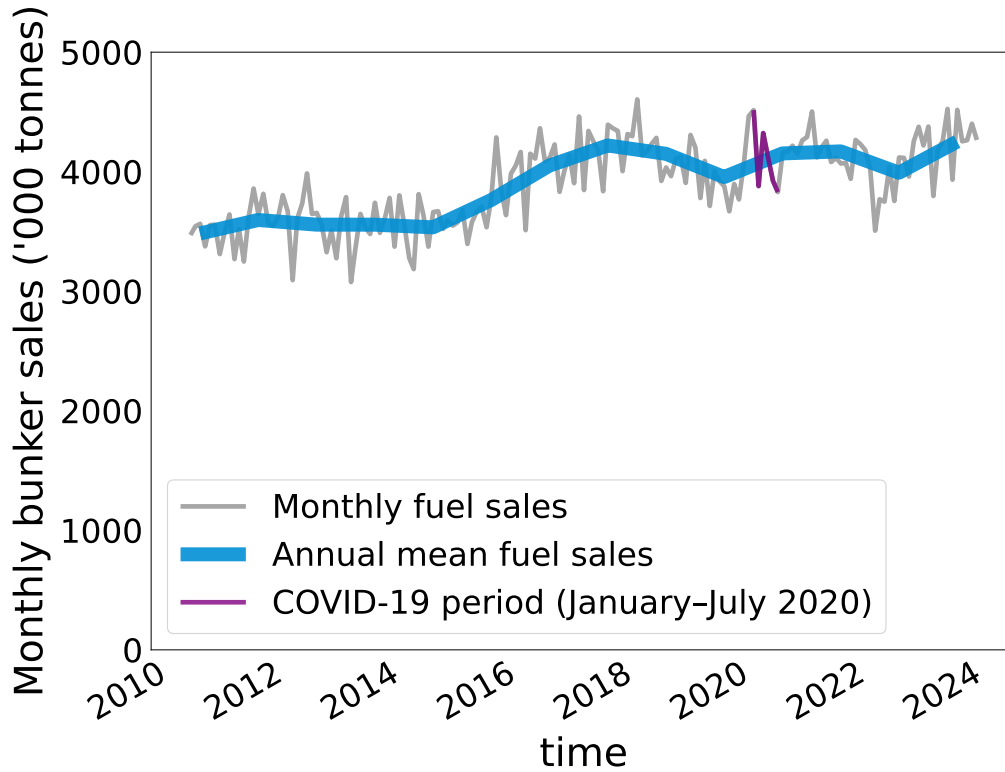


Fig. S1. Total fuel sales at the Port of Singapore have been generally increasing

Our approach to lightning stroke density analysis differs slightly from that of Thornton et al., (2017), in that only the Southern Indian Ocean reference region is used for CAPE–Precip analysis due to its similarity to the Indian Ocean shipping lane in frequency of convection and precipitation during the high-lightning season (November to April). Conducting the same analysis with the Northern Indian Ocean reference region does not alter the conclusions of this analysis. Blue boxes in Figure S2 show regions used for compositing lightning and N_d as a function of distance from the shipping lane.

Over both shipping lane regions, seasonal to subseasonal variability is dominated by the migration of the ITCZ, also called the monsoon, as well as the Madden-Julian Oscillation (MJO). The high lightning season in each region occurs when the ITCZ migrates over the shipping lane before reaching a stable location a few hundred kilometers away. This passage of the ITCZ, on top of periodic MJO-related convection, cause considerable variability in the background within a single high lightning season and across years. For this reason, we analyze the data first on an annual basis, taking an entire high lightning (monsoon) season (Figure 2 in the main manuscript), to complement the more rigorous high resolution (3-hourly) analysis shown in Figure 3 in the main manuscript.

For calculating the anomalous lightning enhancement over the shipping lanes shown in Figure 2B of the main manuscript, we regress out of the lightning stroke density the interannual variations in CAPE, Precipitation, and large scale climate variability represented by the ENSO ONI index. The predicted lightning stroke density using these variables outside of the shipping lane is shown in Figure S3 below.

In both Figure 2B and Figure 3 in the main manuscript, we remove the effects of CAPE and precipitation, which are considered reliable measures of MJO and monsoon activity and intensity (Zhang et al, 2022). These analyses also control for interannual variability of ITCZ strength as well as variations in MJO phase. Moreover, the intraseasonal variability associated with the MJO, shown in Figure S4, has no clear trend since 2020 and thus its specific role in the changes in the lightning enhancement is negligible.

SST-driven fluxes on heat and moisture may also be important for setting the stage for convection to occur and for driving instability; however, the connection between SSTs and lightning is less obvious than that for the more direct measures of instability (CAPE and precipitation) used here. For a more in-depth analysis of the SST-pattern drivers of convection and ITCZ migration in this region, we refer the reader to Zhang et al ?.

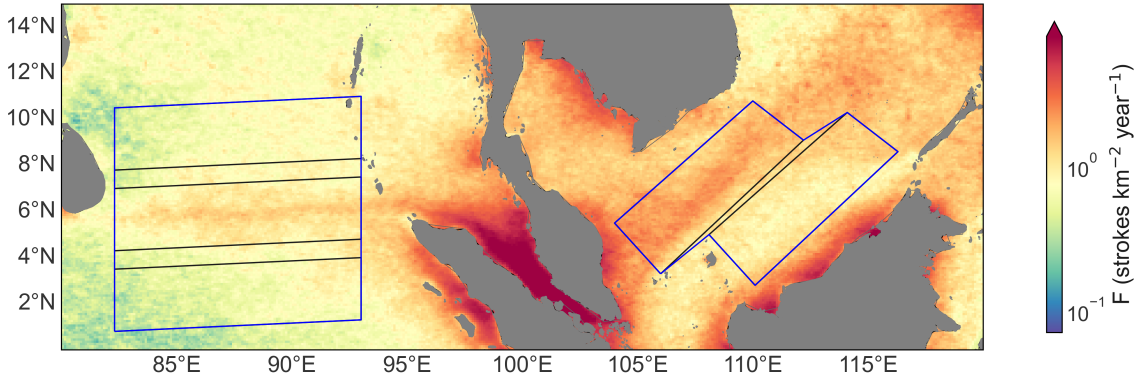


Fig. S2. Climatology as in Figure 1, but with the boxes indicated in black that are used for calculating the shipping lane lightning enhancements as a function of CAPE and Precipitation presented in Figure 3.

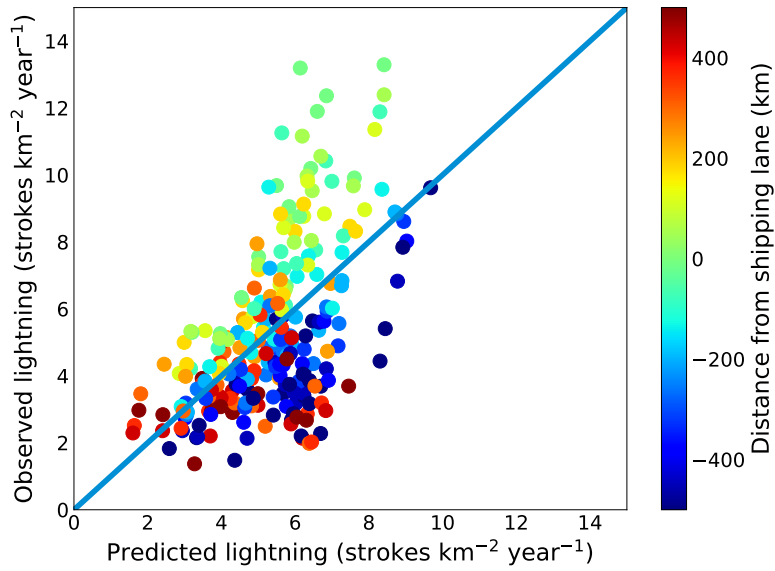


Fig. S3. Observed vs predicted lightning stroke density. Predictions are from linear regression of lightning stroke density against CAPE, precipitation, and ONI. Colors show the distance from the shipping lane. R^2 is 0.33.

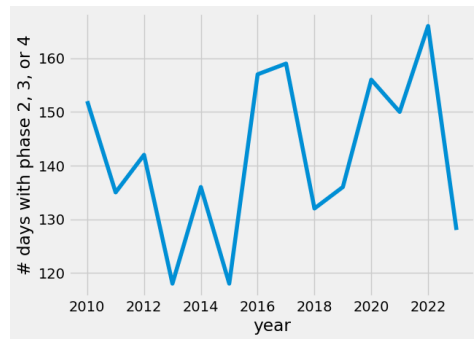


Fig. S4. Number of days with MJO phase 2, 3, or 4 from Realtime Multivariate MJO Index (RMM). This indicator of intraseasonal variability shows no clear trend since 2020

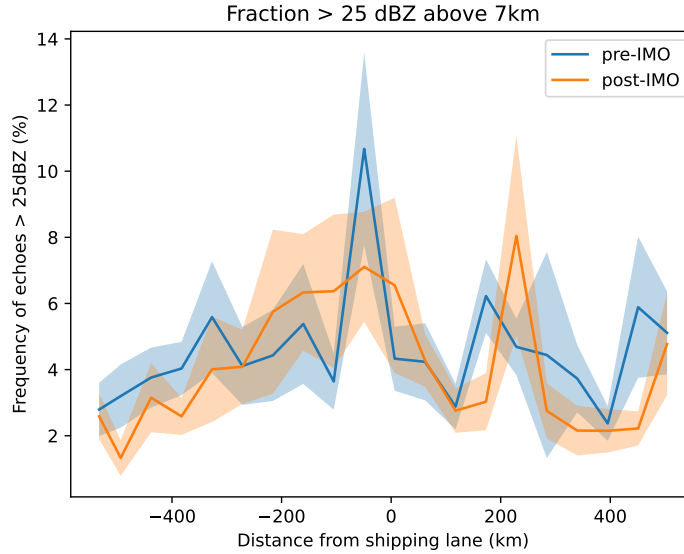


Fig. S5. Frequency of cold echoes (25dBZ or greater, above 8km) from GPM, discussed in Blossey et al (2018) and citations therein as a proxy for lightning. The peak in reflectivity has diminished since the regulation, but weak sampling power does not allow us to confirm this change (the pre-IMO record is restricted GPM’s record, i.e. years since 2016).

We use the GPM precipitation feature database from Chuntao Liu’s group to probe the shipping lane enhancement of cold, strong reflectivity echoes ?. Note that this approach to examining reflectivity is slightly different from that done in Thornton et al. Thornton et al. (2017), but follows that in Blossey et al Blossey et al. (2018). Due to infrequent sampling and small swath width, the reflectivity signal shown here requires very long records to show the effect of the shipping lane (previous studies, such as Blossey et al Blossey et al. (2018), use the full TRMM record, which is well over a decade). Splitting the relatively short (8 year) GPM record of reflectivity into a pre- and post-IMO period therefore greatly reduces the statistical power of the retrievals. Indeed, the peak in reflectivity established over the shipping lane between 2016 and 2019 has diminished (Figure S5). However, the difference between the two periods is not statistically significant (p less than 0.05), and we therefore refrain from concluding that there has or has not been a change to reflectivity above the shipping lanes.

While a correspondence between aerosol optical depth (AOD) and CCN has been documented in some highly polluted regions, this relationship is not established for the typically clean ($AOD < 0.02$) regions of interest here. Therefore, as noted in the main manuscript, we expect that perturbations to CCN in the shipping lane regions is best represented by MODIS N_d retrievals, rather than by AOD because 1) clear sky conditions are rare in this region leading to limited AOD retrievals and consequently limited statistical power, 2) the background AOD is very low, such that an expected perturbation is barely above the limit of detection, and 3) AOD being proportional to aerosol cross sectional area columns does not directly correspond to CCN number at cloud base, the subject of this paper. For example, as shown in Figure S5, AOD estimates from MERRA-2 reanalysis, nudged by both their aerosol model and the limited AOD observations by MODIS, exhibit no observable enhancement over the shipping lanes prior to or after the 2020 IMO regulation. This lack of AOD enhancement is somewhat expected given that ship emissions of aerosol particles are concentrated in smaller, less radiatively active particle sizes [see, e.g., Hobbs et al., Hobbs et al. (2000) and Seppala et al. Seppälä et al. (2021)], statistical sampling is limited by infrequent cloud-free scenes, and that particle scavenging and dilution rates in these regions are relatively high due frequent convection.

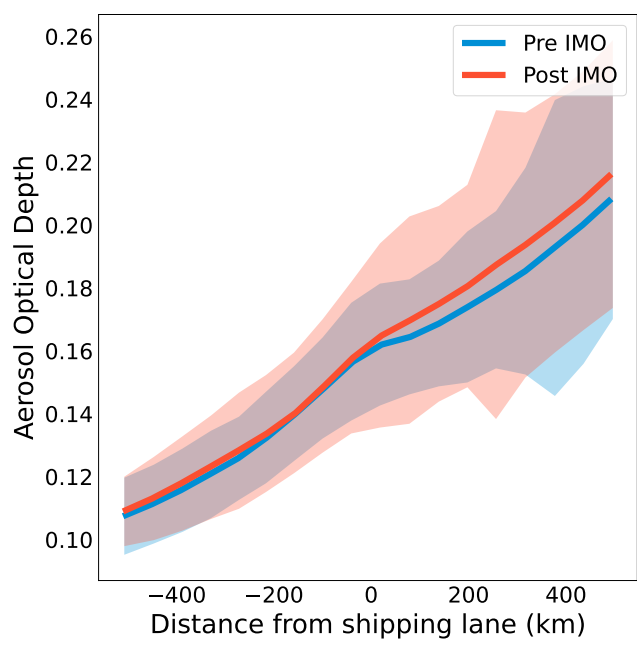


Fig. S6. Mean Aerosol Optical Depth from MERRA-2 as a function of distance from the shipping lane. Shading indicates 95% confidence.

